Biochemical and Biophysical Research Communications 373 (2008) 113–118

Contents lists available at ScienceDirect

Biochemical and Biophysical Research Communications

journal homepage: www.elsevier.com/locate/ybbrc

Mild processing defect of porcine ΔF508-CFTR suggests that ΔF508 pigs may not develop cystic fibrosis disease ☆

Yanli Liu [a], Ying Wang [a], Yong Jiang [a], Na Zhu [a], Haitao Liang [a], Lina Xu [a], Xuechao Feng [a], Hong Yang [a,b], Tonghui Ma [a,b,*]

[a] Membrane Channel Research Laboratory, Northeast Normal University, 5268 Renmin Street, Changchun, Jilin 130024, PR China
[b] Biopharmaceutical Center, Liaoning Normal University, Dalian 116029, PR China

ARTICLE INFO

Article history:
Received 30 May 2008
Available online 12 June 2008

Keywords:
Porcine CFTR
ΔF508 mutation
Processing defect
Transgenic pig model

ABSTRACT

Recent efforts have made significant progress in generating transgenic pigs with the ΔF508-CFTR mutation to model the lung and pancreatic disease of human cystic fibrosis. However, species differences in the processing and function of human, pig and mouse ΔF508-CFTR reported recently raise concerns about the phenotypic consequence of the gene-targeted pig model. The purpose of the present study was to characterize the ΔF508 mutant of porcine CFTR to evaluate the severity of its processing defect. Biochemical and immunofluorescence analysis in transfected COS7 and FRT cells indicated that pig ΔF508-CFTR efficiently targets to the plasma membrane and is present mainly as the mature glycosylated protein. Functional characterization in stably transfected FRT cells by fluorometric and electrophysiological assays supported efficient plasma membrane targeting of pig ΔF508-CFTR. The mild cellular processing defect of pig ΔF508-CFTR suggests that its gene-targeted pig model may not develop the lung and pancreatic phenotypes seen in CF patients.

Cystic fibrosis (CF) is the most common lethal autosomal recessive disease involving multisystem disorders in the Caucasian population [1]. Numerous mutations on the gene encoding cystic fibrosis transmembrane conductance regulator (CFTR), a cAMP-activated epithelial chloride channel, have been identified to be responsible for CF [2]. Deletion of the codon encoding the phenylalanine residue at position 508 (ΔF508) in CFTR appears in one allele of ~90% CF patients. ΔF508 is a processing-defective mutation that causes retention of CFTR at the endoplasmic reticulum [3–5], resulting in Cl^--impermeable cells in various CFTR-expressing organs. Therefore, correction of defective processing of the ΔF508 mutant would benefit the majority of CF patients.

Substantial efforts have been made in the generation of transgenic CFTR-deficient and mutant mouse models manifesting the lung pathology in CF patients for mechanistic and therapeutic studies [6]. However, because of differences in lung physiology between mice and humans, these transgenic mice failed to develop typical lung and pancreatic disease that cause most of the morbidity and mortality in CF patients. Therefore, a large animal transgenic model of ΔF508-CFTR that manifests the human CF lung and pancreatic pathology is desirable for elucidation of disease pathophysiology and for the development and testing of therapies for this devastating disease.

Recent advances were reported in generating transgenic large animal models with ΔF508 and null mutations of CFTR [7,8]. Using a nuclear transfer strategy, Rogers et al. have successfully generated heterozygous transgenic pigs with targeted ΔF508-CFTR mutation [7]. However, a recent study reported by Osedgaad et al. indicated partial cellular processing and significant plasma membrane targeting of porcine ΔF508-CFTR [9], raising concerns about the phenotypic consequences of the ΔF508 pig model. The purpose of this study was to characterize the biochemical, functional and pharmacological properties of porcine ΔF508-CFTR to evaluate the severity of its processing defect.

Methods

cDNA cloning and site-directed mutagenesis of pig CFTR. cDNA sequence encoding full-length porcine CFTR (pCFTR) was cloned

Abbreviations: CF, cystic fibrosis; CFTR, cystic fibrosis transmembrane conductance regulator; NBD, nucleotide binding domain; wt, wild-type; FRT, fisher rat thyroid.

☆ This work was supported by National Natural Science Fund for Distinguished Young Scholars (No. 30325011), National Natural Science Fund (Nos.: 30470405, 30570864, and 30670477), Distinguished Young Scholars Fund of Jilin Province (No. 20030112), and Excellent Young Teachers Program of MOE, PR China, Program for New Century Excellent Talents in University (NCET-07-0406).

* Corresponding author. Address: Membrane Channel Research Laboratory, Northeast Normal University, 5268 Renming Street, Changchun, Jilin 130024, PR China. Fax: +86 431 85099223.
E-mail address: math108@nenu.edu.cn (T. Ma).

0006-291X/$ - see front matter © 2008 Elsevier Inc. All rights reserved.
doi:10.1016/j.bbrc.2008.06.009

from the lung of adult pig (Belgian Landrace strain) by RT-PCR using primers (forward: 5′-CA*GGTACC*ATGCAGAGGTCGCCTCTGG-3′; reverse: 5′-GGC*CTCGAG*CTAAAGTCTTGTTTCTTGCACC-3′) designed according to porcine genomic sequences in two BAC clones (GenBank Accession No. AC092497 and AC092478) containing 5′ end and 3′ end coding sequences corresponding to full-length human CFTR cDNA coding sequence. The cloned pCFTR cDNA was ligated to mammalian expression vector pcDNA3.1Zeo (Invitrogen) to form recombinant plasmid pcDNA3.1Zeo/pCFTR. The cloned pCFTR cDNA was analyzed by extensive DNA sequencing from both directions to obtain the full-length coding sequence. The ΔF508 mutation of pig CFTR was generated in pcDNA3.1Zeo/pCFTR by site-directed mutagenesis to form pcDNA3.1Zeo/ΔF508-pCFTR using a PCR-based strategy as described previously [10].

Generation of pig CFTR NBD2-specific antibodies. Rabbit polyclonal antibodies were raised against the pig CFTR NBD2 (residues Gly-1187—Glu-1475). The pig CFTR NBD2 coding sequence was PCR amplified using primers (sense: 5′-CG*GAATTC*GGCCAGCTTT CAAAGGTTATG-3′ with engineered restriction site EcoRI; antisense: 5′-GC*GTCGAC*CTATTCTTCTGTTTCCTCCTTCAG-3′ with engineered restriction site SalI). The amplified NBD2 fragment was digested with EcoRI/SalI and subcloned into the prokaryotic expression vector pGEX-4T-1 (Amersham) to form expression plasmid pGEX-NBD2. This resulted in a fusion of NBD2 with glutathione *S*-transferase protein. The GST-NBD2 fusion protein was expressed in *Escherichia coli BL21*, affinity-purified on a Glutathione Sepharose 4B column (Sigma), and then injected subcutaneously into New Zealand White rabbits. IgG fraction of the immune serum was purified by Montage™ Antibody Purification Kit (Millipore). The resulting polyclonal antibodies was stored at −70 °C and used at 1:500 dilution.

Immunoblotting and immunofluorescence. COS7 cells were cultured in DMEM supplemented with 10% FBS, 2 mM L-glutamine, 100 U/ml penicillin, and 100 μg/ml streptomycin. The cells were transiently transfected with pcDNA3.1Zeo/pCFTR, pcDNA3.1Zeo/ΔF508-pCFTR, pcDNA3.1/hCFTR, and pcDNA3.1/ΔF508-hCFTR (the two human CFTR plasmids were gifts from Dr. Luis J.V. Galietta) separately using Lipofectamine 2000 (Invitrogen) according to manufacturer's instruction. For immunoblotting, the transfected cells in 6-well plates were harvested 48 h after transfection and membrane-enriched fraction was prepared and used for SDS–PAGE and blotted to PVDF membrane as described [11]. Expression of pig CFTR protein was detected using the polyclonal pig NBD2 antibody and an ECL plus kit (Amersham). For immunofluorescence, the transfected cells in 12-well plates were fixed with 4% paraformaldehyde and permeabilized with 0.1% Triton X-100. Localization of pig wild-type and ΔF508-CFTR in the transfected cells was detected using the pig NBD2 antibody and a rhodamine-labeled goat anti-rabbit IgG secondary antibody (Sigma). Localization of human wild-type and ΔF508-CFTR was detected using the monoclonal antibody M3A7 (AllState) and a rhodamine-labeled goat anti-mouse IgG secondary antibody (Sigma).

Stable transfection. Fischer rat thyroid (FRT) cells were cultured in Coon's modified F12 medium supplemented with 10% fetal bovine serum, 2 mM L-glutamine, 100 U/ml penicillin, and 100 μg/ml streptomycin as described previously [12]. For CFTR functional studies, FRT cells were first stably transfected with the iodide-sensitive green fluorescent analog EYFP-H148Q [13] in pcDNA3.1 vector and selected in 0.75 mg/ml G418 (Invitrogen). Stable cell clone with brightest EYFP fluorescence FRT/EYFP-H148Q was selected and then stably transfected with pcDNA3.1Zeo/pCFTR and pcDNA3.1Zeo/ΔF508-pCFTR separately and selected in 0.75 mg/ml zeocin (Invitrogen). Clonal populations stably co-expressing pig CFTR and EYFP-H148Q were obtained by functional analysis and limited dilution.

Fluorescence plate reader assay. Cells were plated into black 96-well microplates with clear plastic bottoms (Corning-Costar 3904) at 30,000 cells/wells. After 36-h incubation (37 °C, 90% humidity, 5% CO_2), cells were washed three times with PBS (200 ml/wash), leaving 20 μl of PBS after the last wash. Twenty microliters of PBS containing selected CFTR activators or inhibitors at various concentrations were added. After 5 min, 96-well plates were transferred to FluoStar Optima fluorescence plate reader (BMG Lab Technologies) for dynamic fluorescence quenching assay as described previously [12]. Each well was assayed individually for I^- influx by recording fluorescence continuously (200 ms/point) for 2 s (baseline) and then for 12 s after the rapid (<1 s) injection of 120 μl of isomolar PBS in which 137 mM Cl^- was replaced by I^-. I^- influx rates were computed from initial fluorescence versus time-curve slopes (determined by 3rd order polynomial regression) after normalization for total fluorescence (background-subtracted initial fluorescence).

Short-circuit current measurements. Ussing chamber assays of pCFTR-mediated short-circuit current were performed 6–8 days after plating the pCFTR-expressing FRT cells in Snapwell inserts (Corning-Costar 3048) at 500,000 cells/insert. The inserts were mounted in an Ussing chamber system (Physiological Instruments), the basolateral solution contained 130 mM NaCl, 2.7 mM KCl, 1.5 mM KH_2PO_4, 1 mM $CaCl_2$, 0.5 mM $MgCl_2$, 10 mM Na–Hepes, pH 7.3, and 10 mM glucose. In the apical bathing solution, 65 mM NaCl was replaced by sodium gluconate, and $CaCl_2$ was increased to 2 mM. Solutions were bubbled with air continuously and measurements were performed at 37 °C. The basolateral membrane was permeabilized with 250 μg/ml amphotericin B. The hemichambers were connected to a DVC-1000 voltage clamp (World Precision Instruments) via Ag/AgCl electrodes and 1 M KCl agar bridges for recording apical membrane short-circuit chloride currents (I_{sc}).

Whole-cell patch-clamp measurements. Whole-cell patch recording was performed on FRT cells stably expressing wild-type or ΔF508-pCFTR. Patch pipettes were pulled from glass capillaries with an outer diameter of 1.5 mm on a two-stage puller (PP-830, Narishige Co., Ltd., Tokyo, Japan). The resistance between the recording electrode filled with pipette solution and the reference electrode was 3–5 MΩ. The cell membrane was clamped at specified voltages using a patch-clamp amplifier (Axon 700A, Axon Instruments, Foster City, CA) and was sampled and analyzed using a Digidata 1320A interface and a computer with the Clampex and Clampfit software (Clampfit9.2, Axon Instruments). Data were filtered at 500 Hz and digitized at 2000 Hz. For asymmetrical Cl^- condition, the pipette solution contained (in mM): 85 mM aspartic acid, 10 mM EGTA, 20 mM tetraethylammonium-chloride, 10 mM Mg–ATP, 2 mM $MgCl_2$, 5.5 mM glucose, and 10 mM HEPES, pH 7.4, with CsOH. The bath solution contained 119 mM NaCl, 2 mM $MgCl_2$, 1 mM $CaCl_2$, 5 mM glucose, and 5 mM HEPES, pH 7.4 with NaOH. Sucrose (20 mM) was added to the bath solution to prevent the activation of swelling-induced currents. For symmetrical Cl^- condition, the pipette solution contained 10 mM EGTA, 121 mM tetraethylammonium-chloride, 10 mM Mg–ATP, 2 mM $MgCl_2$, 5.5 mM glucose, and 10 mM HEPES, pH 7.4, with CsOH. All the experiments were carried out at room temperature (22–25 °C).

Results

Molecular cloning of porcine CFTR and creation of the ΔF508 mutation

The full-length cDNA sequence encoding porcine CFTR (pCFTR) was cloned from the lung mRNA by RT-PCR amplification using primers designed according to porcine genomic sequences in two overlapping pig genomic BAC clones located on chromosome 7 (GenBank Accession No. AC092497 and AC092478). The cloned

pCFTR cDNA contains a 4446 nucleotides open-reading frame that encodes a 1442 amino acid protein similar in length and composition to those of other mammalian CFTRs. The pCFTR cDNA sequence was deposited in the NCBI GenBank database under Accession No. AY585334. Comparison of protein sequences revealed 92% and 78% overall identities of pCFTR to human CFTR (GenBank Accession No. NP_000483) and mouse CFTR (GenBank Accession No. NP_066388), respectively.

Comparison of the amino acid sequences in the first nucleotide-binding domain (NBD1) indicated 98% identity between pig and human and 86% between pig and mouse CFTRs. The phenylalanine residue at position 508 is conserved in pCFTR [14]. A ΔF508 mutation of pCFTR was generated by site-directed mutagenesis as shown in Fig. 1A.

Mild cellular processing defect of porcine ΔF508-CFTR protein

To characterize the cellular processing of ΔF508-pCFTR protein, we generated a rabbit polyclonal antibody against the NBD2 domain of pCFTR expressed in *E. coli* system. Western blot analysis and immunofluorescence of wild-type pCFTR and ΔF508-pCFTR were performed on transiently transfected COS7 cells cultured at 37 °C. As shown in Fig. 1B, expression of the mature, N-linked glycosylated form (band C) and the immature form (band B) of ΔF508-pCFTR are similar to that of wild-type pCFTR. The C-band/B-band ratio in ΔF508-pCFTR is 3.5 ± 0.7, compared to 0.01 ± 0.004 in human ΔF508-CFTR, and 9.7 ± 1.3 in wild-type pCFTR, indicating that ΔF508-pCFTR is predominantly (78%) in the maturely glycosylated form. Immunofluorescence analysis revealed similar plasma membrane expression patterns of ΔF508-pCFTR and wild-type pCFTR (Fig. 1C, left), supporting efficient plasma membrane targeting of ΔF508-pCFTR. The human ΔF508-CFTR as a control exhibited apparent retention in the endoplasmic reticulum and lack of plasma membrane expression in the transfected cells cultured at 37 °C (Fig. 1C, right). These results indicate a mild cellular processing defect of the ΔF508-pCFTR protein.

Functional analysis shows efficient plasma membrane targeting of porcine ΔF508-CFTR though reduced channel activity

For functional analysis, we established FRT cell lines stably coexpressing the iodide-sensitive GFP mutant EYFP/H148Q [13] with wild-type pCFTR and ΔF508-pCFTR, respectively. Immunoblot analysis of six stably transfected FRT cell clones in each group indicated a similar pattern of predominantly mature CFTR protein with N-linked glycosylation (68% in ΔF508-pCFTR vs. 76% in wild-type pCFTR) as seen in COS7 cells. Selected FRT clones with similar C-band/Na^+,K^+-ATPase ratios of ΔF508-pCFTR (1.46 ± 0.22) and wild-type pCFTR (1.59 ± 0.31) were cultured at 37 °C and assessed by functional analysis.

As shown in Fig. 2A by an I^- influx assay [13], the cAMP-agonist forskolin stimulated remarkable I^- influx into ΔF508-pCFTR-expressing F'RT cells. The maximum forskolin-stimulated I^- influx rate was ~52% of that of wild-type pCFTR. However, the dose-activation curves shown in Fig. 2B indicated a higher EC_{50} of ΔF508-pCFTR for forskolin (2.5 μM vs. 0.25 μM in wild-type pCFTR), suggesting impaired channel gating of ΔF508-pCFTR, as found previously in human and mouse ΔF508-CFTRs [5,15–19]. The impaired channel gating in ΔF508-pCFTR likely results from decreased channel open probability, as reported previously [9].

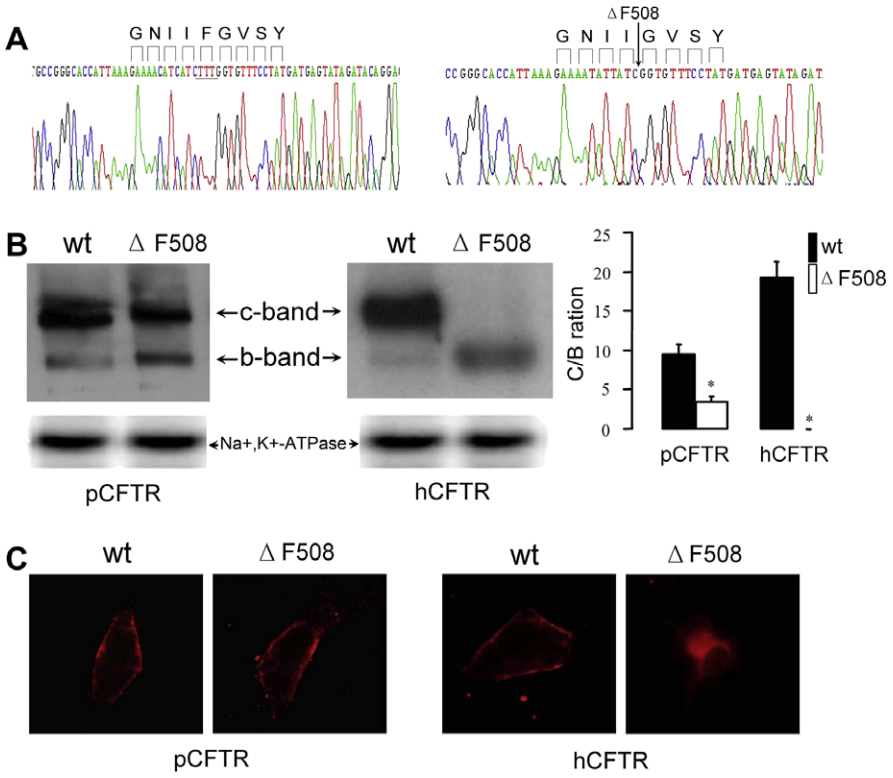

Fig. 1. Generation and biochemical characterization of the ΔF508 mutation in pig CFTR. (A) DNA sequencing results showing the deletion by site-directed mutagenesis of the codon TTT encoding the phenylalanine residue at position 508. (B) Immunoblot analysis of pig wt-CFTR and ΔF508-CFTR (left) with human counterparts as control (right). COS7 cells were transiently transfected with pCDNA3.1 plasmids carrying each of the wild-type and mutant CFTR cDNAs and were incubated at 37 °C for 48 h after transfection. Membrane-enriched fractions of the transfected cells were obtained, and 50 μg protein samples were resolved by SDS–PAGE. The pig blots were probed with an anti-pCFTR (generated against NBD2 domain as described in Methods) polyclonal antibody; the control human blots were probed with an anti-hCFTR monoclonal antibody (M3A7). Data were presented as means ± SE (n = 4–6). $^*P < 0.01$. (C) Immunofluorescence of the transiently transfected COS7 cells. Representative immunostaining of single transfected cells is shown.

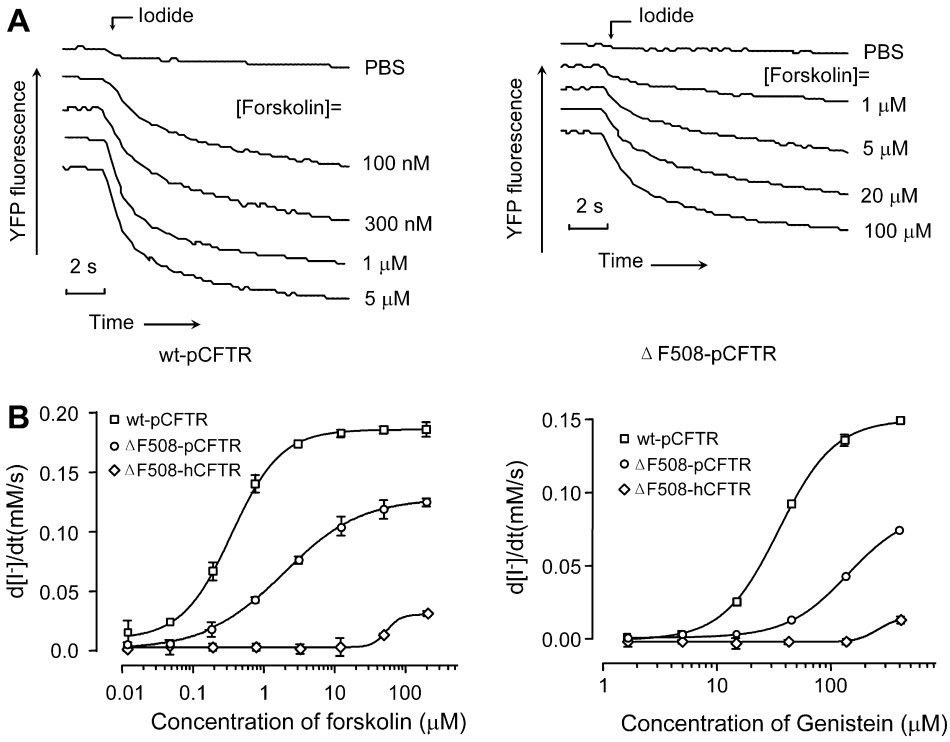

Fig. 2. Functional analysis of pig CFTR and its ΔF508 mutant by fluorometric assay. (A) Representative time courses of EYFP-H148Q fluorescence upon forskolin stimulation in FRT cells stably expressing wt-pCFTR and ΔF508-pCFTR. I^- influx was stimulated in wt-pCFTR (left) and ΔF508-pCFTR (right). (B) Concentration response curves for forskolin (left) and genistein (right) showing remarkably reduced sensitivity of ΔF508-pCFTR to the activators. In all functional studies, the FRT cells were cultured at 37 °C until the measurements.

Fig. 3 shows the Cl^--transport properties of the stably transfected FRT cells cultured at 37 °C by short-circuit current measurements. Forskolin activated wild-type pCFTR and ΔF508-pCFTR-mediated Cl^- currents (I_{sc}) in a dose-dependent manner (Fig. 3A). The maximum forskolin-stimulated current was ~61% relative to the wild-type pCFTR in the assay. EC_{50} was 5 μM in ΔF508-pCFTR vs. 0.5 μM in wild-type pCFTR. After maximum activation by forskolin, 50 μM genistein can further activate the Cl^- current of ΔF508-pCFTR rather than wild-type pCFTR. Comparison of the relative Cl^- currents activated by the same concentrations of forskolin indicated reduced channel function of ΔF508-pCFTR upon cAMP activation (Fig. 3B). These results further demonstrated that majority of ΔF508-pCFTR were targeted to plasma membrane despite the impaired channel gating.

The Cl^- transporting function of ΔF508-pCFTR was further analyzed by whole-cell patch-clamp measurements on the FRT cells stably expressing wild-type and ΔF508-pCFTR. Fig. 4 shows representative data of whole-cell Cl^- currents activated by 5 μM FSK and then inhibited by 30 μM GlyH-101. Both the wild-type (Fig. 4A) and ΔF508-pCFTR (Fig. 4B) are voltage independent and have a liner *I–V* relationship in symmetrical Cl^- solutions. However, the whole-cell Cl^- current of ΔF508-pCFTR was nearly twofold lower than that of cells expressing wild-type pCFTR.

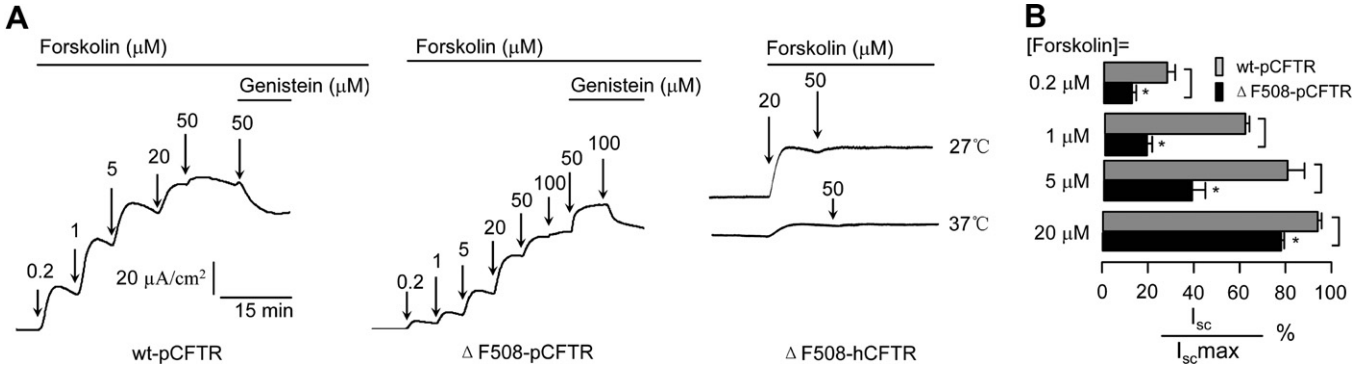

Fig. 3. Functional analysis of pig CFTR and its ΔF508 mutant by short-circuit current assay. (A) FRT monolayers were cultured in Snapwells for 6–8 days at 37 °C. Apical membrane Cl^- currents were measured in Ussing chambers after basolateral membrane permeation with Amphotericin B (250 μg/ml). Currents were recorded continuously, and arrows indicate the addition of forskolin and genistein at various concentrations in FRT cells stably expressing wt-pCFTR (left), ΔF508-pCFTR (middle) and ΔF508-hCFTR (right). (B) Comparison of forskolin activation on wt-pCFTR and ΔF508-pCFTR. Results are expressed as the percentage of the maximum forskolin-stimulated chloride current for each cell line. Data were presented as means ± SE (n = 4–6). $^*P < 0.01$.

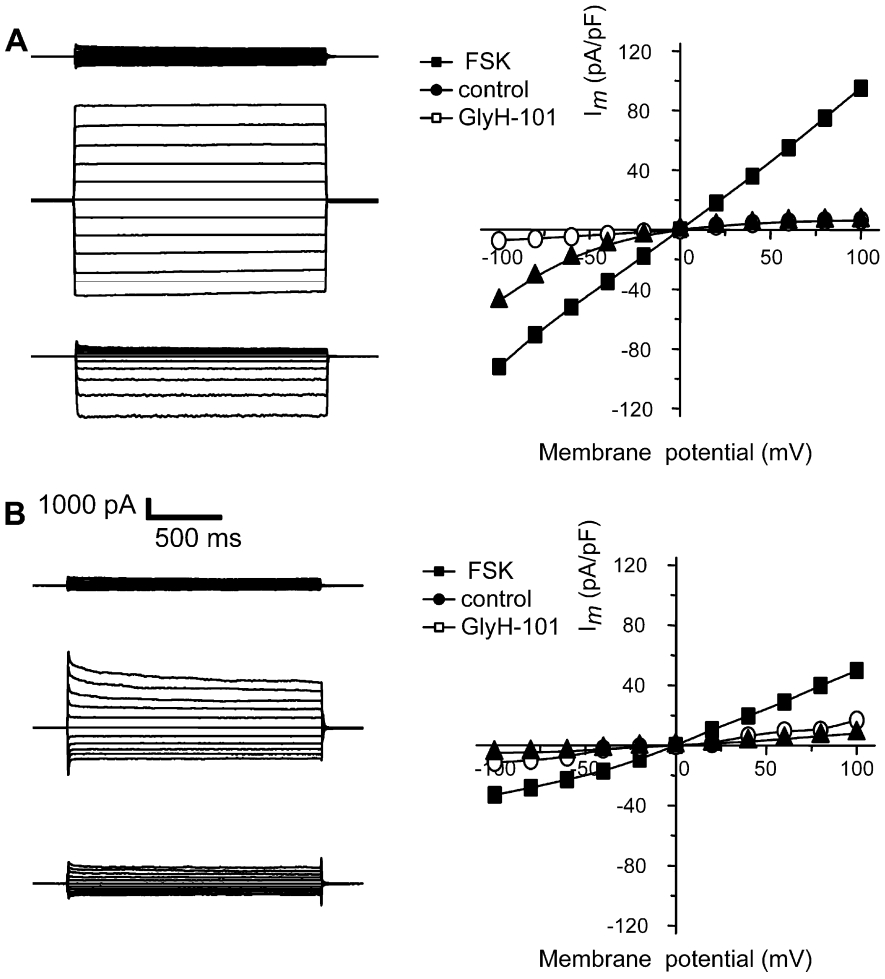

Fig. 4. Altered ΔF508-pCFTR channel gating determined by whole-cell patch-clamp. Representative whole-cell membrane currents and *I–V* relationship evoked by voltages from −100 to 100 mV (20 mV increment) in FRT cells expressing wild-type pCFTR (A) and ΔF508-pCFTR (B) after stimulation by 5 μM FSK, and then inhibited by 30 μM GlyH-101. Holding potential was 0 mV and inter-pulse duration was 4 s.

Discussion

The present study confirmed the species difference of cellular processing defect in ΔF508-CFTR reported previously [9]. However, our results from immunofluorescence, biochemical, and electrophysiological measurements show a substantially more mild ΔF508-pCFTR processing defect than previously reported. Our biochemical analysis indicated a predominant mature N-linked glycosylated form of ΔF508-pCFTR at 37 °C, consistent with the plasma membrane expression pattern of ΔF508-pCFTR that was similar to that in wild-type porcine and human CFTRs.

Functional analysis in stably transfected FRT cells cultured at 37 °C supported efficient plasma membrane targeting of ΔF508-pCFTR. Relative to the wild-type pCFTR, the maximum forskolin-stimulated conductance was ~52% in fluorometric assay (Fig. 2) and ~61% in short-circuit current assay (Fig. 3), which was remarkably higher than 25.6% in Ussing chamber studies reported previously [9]. Moreover, ΔF508-pCFTR produced significantly more current than low temperature-corrected ΔF508-hCFTR upon maximum forskolin-stimulation (Fig. 3A), further supporting efficient plasma membrane targeting of ΔF508-pCFTR.

The differences between our biochemical and immunofluorescence results on ΔF508-pCFTR maturation and those of Ostedgaard et al. may relate, in part, to different antibodies used in the experiments and to different analysis methods. We used a polyclonal antibody against the purified NBD2 domain of porcine CFTR for direct immunoblot analysis, whereas Ostedgaard et al. used a human CFTR antibody for visualization of pig ΔF508-CFTR by immunoprecipitation and in vitro phosphorylation. The differences in Ussing chamber results may be due to the very different systems studied. Ostedgaard et al. using virally infected human CF airway cell cultures, which may process pig ΔF508-CFTR differently from native cells or various transfected cell lines. When available, it will be important to study pig ΔF508-CFTR processing and function in airway epithelial cells derived from homozygous ΔF508 pigs.

Previous patch-clamp studies by Ostedgaard et al. demonstrated decreased open probability (impaired gating) of pig, human and mouse ΔF508-CFTRs, with unchanged single channel conductance [9]. Our functional studies are consistent with these findings, with impaired channel gating of ΔF508-pCFTR as indicated by reduced sensitivity to forskolin in fluorometric (EC_{50} ~2.5 μM vs. 0.25 μM in wild-type pCFTR) and short-circuit current (EC_{50} ~5 μM vs. 0.5 μM in wild-type pCFTR) assays. Whole-cell patch-clamp analysis also indicated a nearly twofold lower Cl^- current in ΔF508-pCFTR compared to wild-type pCFTR, supporting reduced open probability of ΔF508-pCFTR.

The reason that pig ΔF508-CFTR has mild cellular processing defect remains to be determined. Previous studies demonstrated that the cellular processing defect of ΔF508-hCFTR can be significantly rescued by second-site mutations in the nucleotide binding domain 1 (NBD1) signature motif region [20,21]. The identified revertant mutations I539T, G550E, and R555K each partially res-

cued the processing defect of human ΔF508-CFTR. However, none of the three amino acids is changed in pig CFTR in the core signature motif LSGGQ region. Actually amino acid sequence of a wider region from I471 to Q634 in the NBD1 of the cloned pig CFTR is identical to that of human CFTR. Therefore, the mild cellular processing defect of pig ΔF508-CFTR seems unrelated to rescuing variations in the NBD1 LSGGQ signature motif region and warrants further investigation.

The present study confirmed the species difference in cellular processing of ΔF508-CFTR reported by Ostedgaard et al. [9]. However, our results indicated rather mild processing defect of ΔF508-pCFTR compared with their studies. It was estimated that plasma membrane targeting of 10% ΔF508-CFTR protein could avoid the CF phenotype in human subjects [22]. The mild processing defect of porcine ΔF508-CFTR suggests that the transgenic ΔF508-CFTR pig model [7] may not develop the desired CF phenotypes.

Acknowledgments

We thank Dr. Alan Verkman for helpful discussions and Chatchai Muanprasat for technical assistance in Ussing chamber assays.

References

[1] F.S. Collins, Cystic fibrosis: molecular biology and therapeutic implications, Science 256 (1992) 774–779.
[2] J.L. Bobadilla, M. Macek Jr., J.P. Fine, P.M. Farrell, Cystic fibrosis: a worldwide analysis of CFTR mutations—correlation with incidence data and application to screening, Hum. Mutat. 19 (2002) 575–606.
[3] R.R. Kopito, Biosynthesis and degradation of CFTR, Physiol. Rev. 79 (1999) S167–S173.
[4] S.H. Cheng, R.J. Gregory, J. Marshall, S. Paul, D.W. Souza, G.A. White, C.R. O'Riordan, A.E. Smith, Defective intracellular transport and processing of CFTR is the molecular basis of most cystic fibrosis, Cell 63 (1990) 827–834.
[5] W. Dalemans, P. Barbry, G. Champigny, S. Jallat, K. Dott, D. Dreyer, R.G. Crystal, A. Pavirani, J.P. Lecocq, M. Lazdunski, Altered chloride ion channel kinetics associated with the delta F508 cystic fibrosis mutation, Nature 354 (1991) 526–528.
[6] B.R. Grubb, R.C. Boucher, Pathophysiology of gene-targeted mouse models for cystic fibrosis, Physiol. Rev. 79 (1999) S193–S214.
[7] C.S. Rogers, Y. Hao, T. Rokhlina, M. Samuel, D.A. Stoltz, Y. Li, E. Petroff, D.W. Vermeer, A.C. Kabel, Z. Yan, L. Spate, D. Wax, C.N. Murphy, A. Rieke, K. Whitworth, M.L. Linville, S.W. Korte, J.F. Engelhardt, M.J. Welsh, R.S. Prather, Production of CFTR-null and CFTR-DeltaF508 heterozygous pigs by adeno-associated virus-mediated gene targeting and somatic cell nuclear transfer, J. Clin. Invest. 118 (2008) 1571–1577.
[8] X. Sun, Z. Yan, Y. Yi, Z. Li, D. Lei, C.S. Rogers, J. Chen, Y. Zhang, M.J. Welsh, G.H. Leno, J.F. Engelhardt, Adeno-associated virus-targeted disruption of the CFTR gene in cloned ferrets, J. Clin. Invest. 118 (2008) 1578–1583.
[9] L.S. Ostedgaard, C.S. Rogers, Q. Dong, C.O. Randak, D.W. Vermeer, T. Rokhlina, P.H. Karp, M.J. Welsh, Processing and function of CFTR-DeltaF508 are species-dependent, Proc. Natl. Acad. Sci. USA 104 (2007) 15370–15375.
[10] E.Y. Chen, M.C. Bartlett, T.W. Loo, D.M. Clarke, The DeltaF508 mutation disrupts packing of the transmembrane segments of the cystic fibrosis transmembrane conductance regulator, J. Biol. Chem. 279 (2004) 39620–39627.
[11] Y. Wang, M.C. Bartlett, T.W. Loo, D.M. Clarke, Specific rescue of cystic fibrosis transmembrane conductance regulator processing mutants using pharmacological chaperones, Mol. Pharmacol. 70 (2006) 297–302.
[12] T. Ma, L. Vetrivel, H. Yang, N. Pedemonte, O. Zegarra-Moran, L.J. Galietta, A.S. Verkman, High-affinity activators of cystic fibrosis transmembrane conductance regulator (CFTR) chloride conductance identified by high-throughput screening, J. Biol. Chem. 277 (2002) 37235–37241.
[13] L.V. Galietta, S. Jayaraman, A.S. Verkman, Cell-based assay for high-throughput quantitative screening of CFTR chloride transport agonists, Am. J. Physiol. Cell Physiol. 281 (2001) C1734–C1742.
[14] J.M. Chen, C. Cutler, C. Jacques, G. Boeuf, E. Denamur, G. Lecointre, B. Mercier, G. Cramb, C. Ferec, A combined analysis of the cystic fibrosis transmembrane conductance regulator: implications for structure and disease models, Mol. Biol. Evol. 18 (2001) 1771–1788.
[15] C.M. Haws, I.B. Nepomuceno, M.E. Krouse, H. Wakelee, T. Law, Y. Xia, H. Nguyen, J.J. Wine, Delta F508-CFTR channels: kinetics, activation by forskolin, and potentiation by xanthines, Am. J. Physiol. 270 (1996) C1544–C1555.
[16] T.C. Hwang, F. Wang, I.C. Yang, W.W. Reenstra, Genistein potentiates wild-type and delta F508-CFTR channel activity, Am. J. Physiol. 273 (1997) C988–C998.
[17] F. Wang, S. Zeltwanger, S. Hu, T.C. Hwang, Deletion of phenylalanine 508 causes attenuated phosphorylation-dependent activation of CFTR chloride channels, J. Physiol. 524 (Pt 3) (2000) 637–648.
[18] D.J. Davidson, F.M. Kilanowski, S.H. Randell, D.N. Sheppard, J.R. Dorin, A primary culture model of differentiated murine tracheal epithelium, Am. J. Physiol. Lung Cell. Mol. Physiol. 279 (2000) L766–L778.
[19] T.J. Kelley, K. Thomas, L.J. Milgram, M.L. Drumm, In vivo activation of the cystic fibrosis transmembrane conductance regulator mutant deltaF508 in murine nasal epithelium, Proc. Natl. Acad. Sci. USA 94 (1997) 2604–2608.
[20] A.C. DeCarvalho, L.J. Gansheroff, J.L. Teem, Mutations in the nucleotide binding domain 1 signature motif region rescue processing and functional defects of cystic fibrosis transmembrane conductance regulator delta f508, J. Biol. Chem. 277 (2002) 35896–35905.
[21] J.L. Teem, M.R. Carson, M.J. Welsh, Mutation of R555 in CFTR-delta F508 enhances function and partially corrects defective processing, Receptors Channels 4 (1996) 63–72.
[22] L.G. Johnson, J.C. Olsen, B. Sarkadi, K.L. Moore, R. Swanstrom, R.C. Boucher, Efficiency of gene transfer for restoration of normal airway epithelial function in cystic fibrosis, Nat. Genet. 2 (1992) 21–25.